N70 32944

NASA TECHNICAL MEMORANDUM

NASA TM X-52856

NASA TM X-52856

CASE FILE COPY

PRELIMINARY RESULTS OF SERT II SPACECRAFT POTENTIAL MEASUREMENTS USING HOT WIRE EMISSIVE PROBES

by Sanford G. Jones, John V. Staskus,
and David C. Byers
Lewis Research Center
Cleveland, Ohio

TECHNICAL PAPER proposed for presentation at
Eighth Electric Propulsion Conference sponsored by the
American Institute of Aeronautics and Astronautics
Stanford, California, August 31-September 2, 1970

PRELIMINARY RESULTS OF SERT II SPACECRAFT POTENTIAL MEASUREMENTS USING HOT WIRE EMISSIVE PROBES

by Sanford G. Jones, John V. Staskus, and David C. Byers

Lewis Research Center
Cleveland, Ohio

TECHNICAL PAPER proposed for presentation at

Eighth Electric Propulsion Conference
sponsored by American Institute of Aeronautics and Astronautics
Stanford, California, August 31-September 2, 1970

NATIONAL AERONAUTICS AND SPACE ADMINISTRATION

PRELIMINARY RESULTS OF SERT II SPACECRAFT POTENTIAL MEASUREMENTS USING HOT WIRE EMISSIVE PROBES

Sanford G. Jones, John V. Staskus, and David C. Byers
Lewis Research Center
National Aeronautics and Space Administration
Cleveland, Ohio

E-5799

Abstract

Data from the SERT II spacecraft was used to study the variation of spacecraft and ion beam potential with respect to space potential as a function of ion thruster and orbital parameters. Measurements were obtained using floating hot wire emissive probes. Spacecraft potentials of -6 to -11 V with the thruster not operating and -12 to -28 V with the thruster at maximum beam (255 mA) were obtained. The spacecraft potential variations were a function of orbital position. The effect, on spacecraft and ion beam potentials, of varying the ion thruster neutralizer to spacecraft potential was determined. The ion beam-neutralizer potential difference was found to be constant for spacecraft-space potentials from -77 to 0 V with constant neutralizer emission current. Radial potential profiles of the ion beam were also obtained for various spacecraft conditions.

Introduction

The SERT II spacecraft was launced on February 3, 1970. The primary purpose of SERT II was a long duration (6 months) test of a mercury ion thruster.[1] A secondary objective was the investigation of the interaction between the ion thruster, the spacecraft and the ambient space environment. Certain on-board experiment data[2] and the overall spacecraft performance could be affected by the existence of a potential difference between the spacecraft and the plasma (hereinafter called $V_{S/C}$). The thruster and neutralizer performance and lifetime[3,4] are directly related to $V_{S/C}$. In addition, solar cell performance can be strongly influenced by the value of $V_{S/C}$.[5,6] Operation of a solar-electric spacecraft can also influence the ambient space plasma in a variety of ways.[2,5,7,8] Data concerning local electron temperatures and density should be taken outside the plasma sheath surrounding the spacecraft.

The potential difference between the spacecraft and space arises in part from the requirement that the net current to the spacecraft from the space plasma be zero. The magnitude and polarity of $V_{S/C}$ is a function of many variables of the spacecraft and the local plasma conditions.[7,9] The polarity and configuration of the solar cells strongly influence the value of $V_{S/C}$. For example, on two OGO spacecraft $V_{S/C}$ increased from -15 to -2 V when the solar cell tabs were insulated from the space plasma.[2] Thruster operation conditions such as beam current also strongly affect $V_{S/C}$. Neutralizer parameters such as neutral propellant flow and anode keeper voltage can affect $V_{S/C}$. Such neutralizer parameters also affect the potential difference between the ion beam potentials and the neutralizer potential. The value of beam potential can strongly affect the interaction between the beam and space plasma as well as influence the neutralizer lifetime.[3] As pointed out in Ref. 7, beam to neutralizer potentials could be such as to allow large circulating currents between the ion beam and the spacecraft. Such currents could produce magnetic fields which could affect the local space plasma.

The above remarks indicate the desirability of control of $V_{S/C}$. For example, some electrostatic measurements would best be taken if $V_{S/C}$ were near zero,[2,8,9] a situation of minimum electrostatic influence. It has been suggested that this could be done with a bias supply between the spacecraft ground and the neutralizer. Accordingly, an experiment to verify that such a bias supply could be used to control the spacecraft potential was incorporated into the SERT II spacecraft.

This paper presents measurements of spacecraft and beam potentials obtained from various emissive probe measurements. The results of a neutralizer bias experiment on board the SERT II spacecraft is also presented. The data was obtained over a period of several weeks beginning on February 9, 1970 and includes data obtained during the solar eclipse on March 7, 1970.

Instrumentation

Data for the study of the interaction between the ion thruster, the spacecraft, and the ambient space environment was obtained using floating hot wire emissive probes[10,11] and a neutralizer bias supply (Appendix B). Two slightly different types of hot wire probes were employed.[11] The first was a "space probe" which was mounted on a boom extending 1.5 M from the spacecraft (Fig. 1). This probe was used to measure $V_{S/C}$ and extended in the direction of the spacecraft velocity vector, thereby avoiding the effects of any spacecraft wake.[12] This probe was operated continuously. Two other "beam" probes (almost identical in construction) were used to measure the potential of the ion beam of each thruster relative to the spacecraft. These "beam" probes were swept by means of ground command across the exit plane of either the active or passive thruster (Fig. 1). Beam probe 1 was swept across thruster 1. Beam probe 2 was swept across thruster 2. Details of the construction, theory of operation, data accuracy and calibration of the probes are provided in Ref. 11. However, a brief summary is provided in Appendix A. It should be noted that the measurements had an uncertainty of approximately 1.3 and 1.8 V, respectively, for the space and beam probe due to the quantization of the data by the telemetry system. A brief description of the spacecraft and ion thruster is presented in Appendix B.

Results and Discussion

The results from the SERT II flight emissive probe measurements are discussed below. The first section, "Passive Spacecraft," gives the results obtained at the beginning of the mission, prior to operation of the thrusters. Also presented are the data obtained when the thruster was turned off briefly due to a solar eclipse after about 500 hours of thruster operation.

The second section, "Active Spacecraft," presents data obtained during normal operation of each thruster. Thruster operating data is contained in Ref. 13. Also included are the results obtained during the start-up of each thruster. During these periods, the ion beam current and other thruster parameters were varied.

Section three, "Neutralizer Bias Experiment," contains the data obtained when a bias was applied between the neutralizer and spacecraft ground.

All of the flight data is presented using the ambient plasma as the zero potential reference. In general, each graph of flight data is an average of several orbits of data obtained over several weeks. As such, the effects of long term (seasonal) variations in ionospheric properties and/or probe characteristics have not been considered.

The ground data was obtained during final thermal vacuum testing of the flight spacecraft. The neutralizer emission current I_g, was not measured during these tests due to experiment difficulties. And the beam probe was only operated when the ion thruster was at 100 percent beam (approximately 250 mA). The values of spacecraft potential $V_{S/C}$, were obtained by means of a voltmeter between the spacecraft and the vacuum chamber. This was necessary since, in the ground spacecraft tests, the space probe was not deployed. Previous tests of the prototype spacecraft with a deployed space probe showed that the spacecraft potentials measured with a voltmeter between the spacecraft and vacuum chamber ground agreed with the spacecraft potentials obtained with the space probe within 2 V.

Passive Spacecraft

Space Probe Results

The potentials obtained for the passive spacecraft are shown in Figs. 2(a) and (b) for sunrise and sunset, local time. As indicated in Appendix B, the spacecraft was always within 9° of the terminator and the orbit was always approximately parallel to the Earth's magnetic field. However, the alignment of the spacecraft velocity vector was parallel and antiparallel, respectively, to the Earth's magnetic field for the sunrise and sunset conditions. The mean values are -6.4 and -8 V, respectively, for sunrise and sunset. These values are significantly higher than those obtained on many spacecraft.[14,15] They are, however, consistent with the data reported by Krassovsky[16] and Knudsen[17] who reported potentials of -6 to -15 V. The orbital variations in spacecraft potential will be discussed later in the section. As indicated in Appendix C, the potential of a passive spacecraft is usually on the order of a few tenths of a volt. The results shown in Figs. 2(a) and (b) are higher by more than an order of magnitude.

The net current to the spacecraft must be zero. In Appendix C it is shown that the net ion current to the spacecraft is equal to the ram ion current and is on the order of 0.24 mA. This result was obtained using an electron number density, N_e, of 2×10^4 particles/cm^3 (Ref. 18) and assuming charge and temperature equilibrium. By equating the ram ion current to the electron current collected, an expression can be derived for the electron collection area of the spacecraft. The only areas available for electron collection are those near (within a few electron volts) or above plasma potential. For the potentials shown in Figs. 2(a) and (b), the only areas on the spacecraft capable of being near or above plasma potential are the exposed connections on the solar array (Appendix B). All other potentials were shielded from the space plasma. Appendix B gives the measured area of the exposed connections of the solar array which is above plasma potential as a function of the spacecraft to space potential difference. A close correlation between the measured and calculated electron collecting areas would indicate that the high spacecraft potentials obtained are primarily due to the exposed leads on the solar array.

For the SERT II spacecraft, neglecting rf, magnetic and photoemission effects, equating of ion and electron currents require that (Appendix C)

$$eA_i N_i S_{S/C} = eA_e N_e \left(\frac{kT_e}{2\pi M_e}\right)^{1/2} \qquad (1)$$

where

A_e effective electron collection area, M^2

k Boltzmann constant, J/°K

N_e N_i = Particle number density, particles/M^3

M_e electron mass, kg

e electron charge, C

T_e electron temperature, °K

$S_{S/C}$ spacecraft velocity M/sec

A_i ion collection area, M^2

The left side of Eq. (1) is the ram ion current. The right side is the electron current collected by the effective collection area. The values of electron temperature, T_e, at sunrise and sunset were found in Ref. 18 to be 1700° and 2100°K, respectively. It is noted that these values of T_e are for the vernal equinox period of 1965. If these values are used, the above equation reduces to the condition that:

A_e 1.18 M^2 for a spacecraft at sunrise (T_e = 1700° K)

A_e 1.08 M^2 for a spacecraft at sunset (T_e = 2100° K)

The measured and calculated electron collection areas are tabulated in Table I. The results indicate that the measured areas are approximately 40 percent of the calculated areas. This disparity between the two is possibly due to the existence of a plasma sheath surrounding the collecting area. The large negative potentials are, however, concluded to be due to the presence of exposed solar cell wiring at relatively high (±36 V with respect to the spacecraft) positive potentials. In addition, the variations of spacecraft potential with sunrise or sunset are consistent with diurnal variations in electron temperatures.

Figs. 2(a) and (b) show that the spacecraft potentials varied slightly with orbital position. In general, for the sunrise condition, the spacecraft potential was constant at all latitudes except between 55° and 90° south geomagnetic latitude where a slight decrease (more negative) occurred. At sunset, the spacecraft potential was a maximum at the geomagnetic equator and increased (became less negative) towards the poles. The variations, in both cases, are a maximum of ±1 telemetry count (±1.3 V). Attempts were made to correlate the orbital changes in spacecraft potential at sunrise and sunset with the corresponding variations in N_e and T_e using the data from Explorer XXII.[18] It was not possible to make a direct correlation due to the rapid changes in N_e and T_e with time at sunrise and sunset. It was determined, however, that the orbital variations in spacecraft potentials were well within those explainable by small changes in T_e (and perhaps changes in N_e due to its effect on the effective electron collection area). It is to be noted that the observed variation in spacecraft potential might also be due to error in probe measurements caused by plasma density variations.[10]

Data was obtained which allowed a determination of the maximum contribution of photoemission to the spacecraft potential. Fig. 3(a) and (b) shows spacecraft potential data obtained during the solar eclipse of March 7, 1970 (after about 500 hr of thruster operation). The spacecraft was in the Moon's shadow for two periods of about 15 minutes each. As Fig. 3(a) and (b) indicate, the spacecraft potential did not change during the eclipse period within the uncertainty of the measurement. This indicates that the effect of photoemission on spacecraft potential was negligible.

Beam Probe Results

Beam probes 1 and 2 were operated prior to turn-on of the thruster systems. The results of these beam probe sweeps are shown in Fig. 4 along with space probe data obtained at the time of the beam probe sweeps. Under this condition, the beam probes were being used as space plasma ($N_e \simeq 10^4$ to 10^6 particles/cm^3) potential measuring probes. These probes, as indicated in Appendix A, were designed for operation in a plasma of 10^7 to 10^{10} particles/cm^3 density. The beam probe data are shown as a function of the angle φ between the probe position and the spacecraft velocity vector (Fig. 1). The values of φ over which beam probe 1 and 2 could be swept were ±6 to 180° and 0 to ±174°, respectively (Fig. 1).

Fig. 4 shows that the potentials measured by the two beam probes were constant and identical over a large range of φ. The potential of beam probe 1 (orbit raising thruster) decreased one telemetry count (~1.8 V) at absolute values of φ greater than 110 degrees. It is possible that at these angles beam probe 1 was in the wake of its own support structure. The minimum absolute value of φ that could be attained by beam probe 1 was 6 degrees. This angle was larger than that at which beam probe 1 would have pointed directly at the support structure of beam probe 2 (Fig. 1). It is possible that this is why no evidence of a wake effect occurred on beam probe 1 at small values of φ.

Fig. 4 also shows that the beam probe potentials were one telemetry count (~1.8 V) less than the space probe potential. It is uncertain if this difference is due to telemetry uncertainty or the previously mentioned off design operation of the beam probes. This result is, however, consistent with the view that a sheath surrounds the spacecraft. Such a sheath would probably have a thickness on the order of the Debye length (~4 cm). The beam probes are a maximum of about +12 cm from the thruster, but if they were in the wake or sheath of the spacecraft, the potentials measured would be slightly lower than those of the space probe. This was the case for the data of Fig. 4.

Active Spacecraft

This section presents the space and beam probe voltages obtained with an operating thruster. As with a passive spacecraft, the equilibrium potential of a spacecraft with operating ion thruster(s) (active spacecraft case) is determined by the current interchange between the spacecraft and the ambient space plasma. The various potentials will adjust to provide zero net current to the spacecraft. However, for the SERT II spacecraft, the ion beam current (~0.25 A), and hence the minimum neutralizer emission current are far in excess of any other currents existing between the spacecraft and the ambient space plasma. The ram ion current was calculated to be ~0.24 mA. As a result, for spacecraft with operating ion thruster(s), the equilibrium potential is probably largely determined by the interaction between the ion thruster currents and the ambient space plasma. Many of the space plasma, ion beam and spacecraft interactions which could occur are discussed in Ref. 7. These interactions include those between the space plasma, the ion beam, and the spacecraft and possibly between the neutralizer, spacecraft and space plasma.

Results of both ground and flight tests are presented. Several differences existed between ground and flight tests which relate to possible interactions. These are:

(1) The background neutral and plasma densities existing during ground tests were greater than those in space by more than three orders of magnitude. As the background plasma density decreases, the interaction between the space plasma and the ion beam may decrease.[7]

(2) The interaction distance between the ion beam and the local background plasma is limited in ground tests by the vacuum facility dimensions. Ref. 7 indicated that the space plasma - ion beam interaction distances are of order 10 M or greater.

(3) In flight, the spacecraft is exposed to variation (positional, seasonal, etc.) of local plasma parameters not experienced in ground tests.

Space Probe Results

Fig. 5 shows the variation of the spacecraft potential with geomagnetic latitude at sunrise and sunset. As stated previously, the spacecraft velocity vector was nearly parallel and antiparallel to the Earth's magnetic field at sunrise and sunset, respectively. At sunrise, the spacecraft potential was near maximum value at the geomagnetic equator and decreased towards the poles. This trend was essentially reversed at sunset. It is also seen that considerable variation existed, especially over the south geomagnetic pole. The mean value of

spacecraft potential in both cases was 20 to 22 V negative. This is close to the ground test value of -14 V. The maximum value of spacecraft potential shown on Fig. 5 is -28 V. These results are lower than those reported by Cybulski, et al. and Hunter for the SERT I and ATS-IV vehicle, respectively.[19,20] Cybulski reported spacecraft potentials of between 40 and 150 V positive. However, the SERT I potential data was obtained indirectly from E-field meter measurements. And as concluded by Sellen and Cybulski in Ref. 21, the E-field measurements were strongly influenced by particle current collection from the ambient space plasma. In Ref. 20, Hunter reported spacecraft potentials of -43 and -132 V. However, he indicated that the neutralizer might have been emission limited. It is is to be noted that preliminary data, which is not presented, has been obtained which indicates spacecraft potentials of greater than 60 V negative during some orbits.

Attempts were made to correlate the orbital variations in spacecraft potential with ambient plasma variations observed on the Explorer XXII spacecraft during the vernal equinox of 1965.[18] Except at high southern latitudes during sunrise (where diurnal variation in plasma parameters are rapid), the spacecraft potentials did correlate with changes in the electron number density N_e. As of this writing, it is not definitely known why this correlation exists.

Beam Probe Results

Fig. 6 presents beam probe potentials obtained with an operating thruster during both ground and flight tests. For reference, beam probe potential measurements obtained over the inactive thruster are also included. Only the results obtained when the orbit raising thruster was operated are shown. However, the results for both operating thrusters were similar.

The flight data has been divided into Northern and Southern hemispheric results. The Northern hemispheric data was obtained when the spacecraft was at geographic latitudes greater than 30°. Similarly, the Southern hemispheric data was obtained when the spacecraft was south of -30° geographic latitude.

Fig. 6 shows the ion beam potentials V_B, as a function of radial distance R, from the axis of the ion beam and the ion beam half angle θ. The half angle is defined as shown in the sketch on the figure. As stated previously, the data was obtained about 12 cm downstream of the thruster accelerator. However, as the probe traversed the ion beam, the axial downstream distance changed slightly. And this variation has been included in calculation of the half angles shown on Fig. 6.

The results for both flight and ground tests are in good agreement. The maximum beam potential remained essentially constant out to a radial distance corresponding to the diameter of the beam forming electrode. The potential then dropped to a plateau at about 13 to 18 cm. This radial distance is at a half angle corresponding to the neutralizer position. The potential difference between the peak and the plateau was approximately constant for all tests and equal to about 40 V. The voltage remained constant out to about R = 35 to 40 cm and then decreased sharply to values below the ambient space potential. For the flight and ground data, respectively, the spacecraft potential was about 20 and 14 V negative with respect to the space potential. It is possible that at large values of R(>40 cm) the beam probes were strongly influenced by the spacecraft's electric fields. It is also seen that the potentials measured by the beam probe adjacent to the inactive thruster were between about 8 and 13 V negative with respect to the local space potential. This is about a factor of two to three times those measured with both thrusters off (Fig. 3). This is in agreement with the view that the beam probes are immersed in the sheath of the spacecraft.

The data of Fig. 6 were used to obtain ion beam to neutralizer potential differences. These are tabulated in Table 2 for R = 0 (beam center) and $R \simeq 17$ cm (neutralizer position). The table shows that the ion beam-neutralizer potential was constant for a fixed value of R and was approximately equal for both flight and ground tests. It is of interest to note that this agreement between ground and flight data exists even though the ambient plasma density during the ground tests was greater than the space plasma density by more than a factor of 10^3. This similarity between ground and flight data indicates that ground test neutralizer lifetime and performance data are probably applicable to flight conditions.

Neutralizer Bias Experiment

The spacecraft contained a power supply which could bias the neutralizer relative to the spacecraft by a nominal 25 or 50 V positive or negative. This neutralizer bias supply was used to investigate whether the spacecraft potential with respect to the space plasma potential could be varied so as to minimize the electrostatic influence of the spacecraft on the space plasma.

Table 3 presents the experimental results at the various neutralizer bias and thruster operating conditions, for both flight and ground test. The flight data has been divided into Northern and Southern hemispheric results as in the section, "Active Spacecraft." The various bias conditions are labeled I through V in order of decreasing positive bias of the neutralizer with respect to the spacecraft. A positive bias is taken to be that situation that exists when the neutralizer is positive with respect to the spacecraft. As previously indicated, the spacecraft, neutralizer, and beam voltages are all given with respect to the local space potential as determined by the ambient probe. It is seen from Table 3 that the flight and ground data are in general agreement.

The spacecraft potential as a function of neutralizer bias with respect to the spacecraft is shown in Fig. 7. The spacecraft equilibrium potential was approximately -20 V in both the Southern and Northern hemisphere and -14 V during ground tests with the neutralizer at spacecraft potential. As indicated previously, preliminary data, which is not presented, has been obtained for which the spacecraft equilibrium potential was greater than -60 V.

When a bias was applied, the equilibrium potential changed. In the Southern hemisphere, and on ground tests, the change in spacecraft potential with bias was approximately equal to the applied

voltage. Similar results were obtained in the Northern hemisphere except that when the negative bias was applied, the spacecraft potential did not become positive but reached a saturation value approximately equal to plasma potential. From the table it is seen that the neutralizer emission current, I_9, in flight was constant for positive biases (cases I and II) but increased for negative biases (cases IV and V) to a maximum of 343 mA. As indicated in Appendix B, this is near the constant current limit of the bias supply. The value of the applied negative bias was thus limited by loading down of the power supply to a maximum of 28.7 V in flight and 39 V on ground tests.

Fig. 8 shows the neutralizer potential as a function of neutralizer to spacecraft potential. It is seen that the potential difference between the neutralizer and the local space plasma remains nearly constant with applied bias in the Southern hemisphere. However, in the Northern hemisphere, variations of as much as 10 V are obtained. The variations were, however, less than the applied bias.

Fig. 9(a) to (c) show the change in beam potential with radial distance R, from the axis of the ion beam and the half angle θ corresponding to that radial distance for various bias conditions.

The results for both flight and ground tests were similar. The beam potentials decreased monotonically with increasingly positive bias. The radial variation of beam voltage was not sensitive to applied bias. It, therefore, seems likely that the beam shape remained unchanged with neutralizer bias. The maximum beam potential for a given bias remained constant out to a radial distance corresponding to the diameter of the beam forming electrode. The potential then dropped to a plateau at about 13 to 18 cm. This radial distance is at a half angle corresponding to the neutralizer position. The voltage then remained constant out to about 35 cm. The potential difference between the peak and the plateau was approximately constant for all biases and equal to about 44 V.

Figs. 8 and 9 can be used to obtain the beam to neutralizer potential as a function of applied neutralizer bias. The results are shown in Figs. 10(a), (b), and (c) for two radial distances. Fig. 10 shows that when the neutralizer was positive with respect to the spacecraft, the beam to neutralizer potential was insensitive to changes in neutralizer bias. On the other hand, when the neutralizer was negative with respect to the spacecraft, the beam to neutralizer potential increased rapidly.

The above data can be used to discuss the nature of the interaction between the spacecraft and the local space plasma during the bias experiment. At bias conditions, where the bulk of the spacecraft was below local plasma potential, the spacecraft potential was easily varied. The change in spacecraft potential was equal to the applied neutralizer bias. And the ion beam and neutralizer emission currents were approximately equal. The effect of the positive bias was to adjust the spacecraft potential so that the ion beam-neutralizer potential difference remained nearly constant (Fig. 10). This is to be expected for constant electron emission current.[22] It should be noted that in flight as the neutralizer bias was increased from zero to +50 V, the area of the exposed connections on the solar array that is above plasma potential decreased to zero.

When the negative biases were applied (cases III and V) the results differed significantly from those of the positive neutralizer bias condition. In flight, the neutralizer emission current I_9, increased while the ion beam current remained constant. As previously noted, no measurements of I_9 were obtained in the ground test. For cases IV and V the difference between the neutralizer emission current and the ion beam current was about 63 and 85 mA, respectively. This result could arise for two reasons. First, when the spacecraft potential became close to plasma potential, large electron currents could be collected by the spacecraft from the space plasma. In this case, the neutralizer injects into the ion beam the sum of the ion beam and the electron current drawn from space in order that the net current to the spacecraft remain zero. Secondly, loop currents could exist from the neutralizer directly to the spacecraft. These two mechanisms are discussed separately below.

In a manner similar to that discussed in the section, "Passive Spacecraft," an estimate can be made of the current to the spacecraft in orbit. The total conductive area of the spacecraft is on the order of 30 M^2. Using a number density N_e, of 2×10^4 particles/cm^2 and an electron temperature T_e, of 2000° K, the electron current that could be collected by the spacecraft is about 7 mA. This current is about an order of magnitude less than the difference between the neutralizer emission and the ion beam current at the two negative bias conditions. This calculated value of electron current is, of course, dependent on the values of N_e, T_e, and spacecraft area used. The values of T_e and N_e are representative of data from a number of spacecraft at a 1000 kM altitude[18,23,24] taken over a wide variety of seasonal conditions and orbital positions. It was noted, however, in Ref. 25 that the electron number density increases with solar activity. The SERT II data was obtained during a period of high solar activity. It is thus possible that the number density used in calculating the collected electron current is lower than the number density existing during the SERT II flight. A number density of about 3×10^5 particles/cm^3 would be required to provide the 85 mA observed with the -27 V bias (case V). The spacecraft collection area of 30 M^2 represents the physical area of the conductive portions of the Agena vehicle. Due to sheath effects, the effective electron collection area might be larger than 30 M^2 by an appreciable amount.

If the space plasma electron number density and the effective electron collection area of the spacecraft are such that the spacecraft collected currents from the space plasma of approximately 68 to 85 mA, then it is expected that the beam-neutralizer potential would change. As indicated previously, the only mechanism for electron emission from the spacecraft, neglecting photoemission which has been shown to be negligible, is emission from the neutralizer into the ion beam. The ion beam-neutralizer potential difference would thus change with electron emission by just that amount necessary to extract the additional electrons. Fig. 11 gives the variation of neutralizer emission

current with ion beam to neutralizer potential. As indicated by Ref. 22, the virtual anode for the neutralizer hollow cathode is probably very close, within 1 to 2 cm, to the neutralizer keeper anode. Thus, the value of beam to neutralizer potential at the half angle corresponding to the neutralizer position has been used. Ground test data from Ref. 22 is also included on Fig. 11. As seen, the flight and ground data curves have the same general form. The results indicate that the beam to neutralizer potential was approximately constant for all applied biases for constant electron emission current.

As indicated, the difference between the ion beam and neutralizer emission current could be attributed to loop currents from the neutralizer to the spacecraft. Such loop currents could exist if the spacecraft were positive with respect to the neutralizer keeper. The value of the spacecraft potential was approximately equal to the keeper voltage for case IV and about 6 V positive with respect to the keeper for case V in the Southern hemisphere. And as indicated in Appendix B, the thruster ground screen, which was always at spacecraft potential, was within 1.2 cm of the neutralizer cathode.

From the above discussion and data, it is not possible to conclusively determine the exact mechanism that causes the increase in I_9 at negative neutralizer biases. It is noted, however, that the existence of a difference in the data over the Southern and Northern hemisphere indicates that the results may be due to currents drawn from the local plasma rather than loop currents to the spacecraft. Ground tests could possibly determine whether significant loop currents between the neutralizer and portions of the spacecraft could exist.

Summary and Conclusions

The emissive probes flown on the SERT II spacecraft in conjunction with the prime ion thruster experiment allowed an investigation of the interaction between the spacecraft, the ion thruster and the ambient space plasma. The parameters measured were the spacecraft-space potential difference and the spacecraft-ion beam potential difference. The probes and the spacecraft digital telemetry system resulted in a maximum measurement uncertainty of approximately 1.8 V.

During periods in which the thruster systems were not operated, the mean SERT II spacecraft equilibrium potential was -6 and -8 V, respectively, for sunrise and sunset. It was concluded that these relatively high negative potentials were due to the presence of exposed solar array interconnections at high (36 V) positive potentials. This was concluded from a comparison of the measured and calculated electron collection area of the solar array. The change in voltage from sunrise to sunset were found to be consistent with small variations in electron temperature. Orbital variation in the spacecraft potential of the order of 5 V were observed. It was not possible to correlate these orbital changes with variations in space plasma parameters such as N_e and T_e. However, the variations were well within those explainable by small changes (on the order of several hundred degrees K) in T_e.

The spacecraft was in the Moon's shadow during the solar eclipse of March 7, 1970. The results of the space probe measurements indicate that photoemission had no detectable effect on spacecraft potentials.

Data obtained during operation of the ion thruster systems indicated mean spacecraft potentials of -20 V for both sunrise and sunset conditions. This result is close to the ground test level of -14 V. Considerable variation in spacecraft potentials with orbital position were observed; on the order of 16 V. These orbital variations were found to roughly correlate with orbital variations in electron number density N_e, data reported by Explorer XXII.

The results of beam potential measurements for flight and ground tests were in general agreement. It was found that the maximum beam potential (measured about 12 cm downstream of the ion thruster accelerator grids) remained constant at about +45 V out to a radial distance corresponding to the diameter of the beam forming grids. The potentials then decreased sharply. The ion-beam to neutralizer potential was found to be equal for flight and ground tests. This was true for the beam axis and at an ion beam half angle corresponding to the ion thruster neutralizer position. This close agreement between flight and ground data indicates that neutralizer lifetime and performance data obtained in ground test is probably applicable to flight conditions.

During portions of the flight a bias power supply was applied between the neutralizer and the spacecraft. The power supply was capable of biasing the neutralizer a nominal 25 or 50 V positive or negative with respect to the spacecraft. The results of the flight verified that such a bias supply could be used to control the spacecraft potential. By applying a suitable bias the spacecraft potential could be easily varied over the range of 0 to -77 V. Therefore it should be possible to control the potential difference between the spacecraft and the space plasma so as to minimize electrostatic influence on the space plasma of an ion thruster bearing spacecraft.

The variation in spacecraft potential was accomplished without noticeable detrimental effect on the thruster system performance. In addition, the ion beam-neutralizer potential difference was constant for all neutralizers biases with a constant neutralizer emission current.

Increases in the neutralizer bias current was obtained at negative bias conditions. It was not possible to conclusively determine whether these increases in neutralizer emission current resulted from large electron currents drawn from the space plasma to the spacecraft or resulted from loop currents from the neutralizer cathode to nearby surfaces at positive potentials.

Appendix A

Each probe system consisted of an emissive assembly and an electronic package (which included the power and signal conditioning). Each instrument had a nominal range of -50 to +100 V.

Ambient Probe

The ambient probe was designed to operate in a low density plasma of 10^4 to 10^6 particles/cm^3. The ambient probe emissive assembly (Fig. 12) consists of a support structure, a shield, and an emitter. The assembly is 7.6 cm long by 0.64 cm in diameter. It weighs approximately 13 g. The emitter is a 1 cm long by 0.076 mm diameter W3%Re filament. The small diameter shield is connected to the emitter through resistors to maintain it at the mean emitter potential. This "shield electrode" close to emitter potential aided in reducing the effect of other nearby surfaces on the probe's potential measuring ability. This was considered necessary since it was determined that for certain ion density-plasma potential combinations, the plasma sheath thickness could be as much as 100 cm. In additon, for a similar reason, the emissive assembly was mounted on the end of a boom (Fig. 13) which, when extended, placed the filament 150 cm (one spacecraft diameter) ahead of the spacecraft surface in orbit. The boom was electrically insulated from the spacecraft. In order to eliminate the requirement for electron collection to measure negative potentials in the low density plasma, the probe is biased by -60 V with respect to the spacecraft.

An electronics package located within the spacecraft supplies filament heating power (2 W) and provides signal conditioning for heater current telemetry and plasma potential telemetry. The package is 7.6 by 7.9 by 14.2 cm, weighs 0.9 kg requires 3.8 W.

The potential measuring circuit consists of a resistor divider network. A fraction (0.0013) of the potential between the filament and spacecraft is conditioned to be presented to telemetry. The probe telemetry output is 0 to 5 V for plasma to spacecraft potentials of -52 to +109.5 V. The digital telemetry system translates the 0 to 5 V to 0 to 61 counts. Thus, the telemetry introduces a measurement uncertainty of ± 1.32 V ($\pm 1/2$ count). A second telemetry output to monitor filament heating current was also obtained.

Ground calibration was accomplished using a low energy argon ion source and a reference probe. The plasma from the ion source was stabilized at a particular ion density and at a potential as close to the vacuum chamber as possible. Current voltage characteristics were generated with the reference probe cold and emissive. The voltage at which the two disagreed was taken as the plasma potential. The flight probe was then swung into the position of the reference probe and the telemetry output recorded. This procedure was repeated for various bias voltages in the range of +50 to -100 V to obtain a curve of telemetry output versus plasma potential.

Beam Probes

The second probe type was designed for operation in a high density plasma of 10^7 to 10^{10} particles/cm^3. This density range is typical of the ion densities in the Hg ion thruster beam. The beam probe emissive assembly (Fig. 14) is 7.6 cm long by 1.3 cm by 0.64 cm and weighs approximately 30 g. The emitter is a 1 cm long, 0.178 mm diameter Ta wire. The shield or "guard electrode" on the tip is electrically floated. The higher density of the ion beam plasma did not necessitate maintaining the shield at filament potential since sheath thicknesses are more than an order of magnitude smaller than in the ambient density range. A probe and a portion of the system circuitry are mounted on an actuator (Fig. 13) adjacent to each thruster. By means of the spacecraft command system, the actuator is energized to sweep the probe tip through the beam. The probe electronics automatically comes on when the sweep begins. The path of the probe tip is a 22 cm radius, 340° arc which passes through a point within 1.75 cm of the beam axis and 12.5 cm from the accelerator plate. The sweep takes 48.5 ± 0.5 sec so that the probe passes across the accelerator in 5 to 6 sec. The beam probe electronics is almost identical to that of the ambient probe. However, the probe bias circuit was not included, since the ion thrust beam particle density is great enough to ensure electron collection by the emitter when the probe potential is positive with respect to the spacecraft. The circuitry also contains protection against high voltage breakdowns (arcs) from the thruster.

The probe potential telemetry range is 0 to 61 counts for -46 to +99 V plasma. This introduces an uncertainty of ± 1.77 V ($\pm 1/2$ count) in the potential measurement. The emitter current telemetry range is 0 to 37 counts for 0 to 3.2 amps rms.

Ground calibration was accomplished in a manner similar to the ambient probe. The ion source used was a mercury ion thruster. The plasma potential was determined by heating the floating reference probe from the nonemissive to the emissive condition and observing the emitted or collected current. The potential at the knee of the current versus voltage curve was taken as the plasma potential.

Appendix B

Detailed descriptions of the SERT II mission and flight objectives are presented in Ref. 1. However, certain spacecraft and ion thruster characteristics that are pertinent to probe measurement ability or spacecraft equilibrium potential are described below.

Spacecraft

The spacecraft is in a nearly circular, 1000 km, retrograde, polar orbit. The inclination angle is 99°. For this orbit, the spacecraft will be in continuous sunlight for 280 days, with the exception of solar eclipses. The orbit, with the Earth's rotation, then results in the spacecraft passing over nearly all points on the Earth at an altitude of 1000 km at either sunrise or sunset, local time. The orbit thus allows a complete map of spacecraft potential variations as a function of both latitude and longitude to be obtained.

In orbit, the orientation of the spacecraft, shown in Fig. 15, is such that the plane of the solar array is aligned along the velocity vector. This, coupled with the orbit inclination, means that the plane of the solar array is also approximately parallel to the Earth's magnetic field. Variations from this position (yaw misalignment) were estimated to be less than 2 degrees. The major axis of the spacecraft is aligned along an

Earth radius line. Deviation from this was less than 2 degrees.

The complete spacecraft in orbit, shown in Fig. 15, consists of two basic cylindrical structures plus a solar array. One structure is 1.1 m long and 1.5 m in diameter. It houses all experiments and accessory instrumentation. This structure is directly attached to the empty Agena rocket. The empty Agena consists of a cylindrical section 4.6 m long and 1.5 m in diameter, plus a 1.5 m section containing the rocket nozzle and solar array. These factors result in an area for ram ion current collection of 10.4 m^2 which is the frontal area of the spacecraft.

A variety of surface coatings resulted from thermal control considerations, i.e., paint, polished Al, and Al tape. All paints used were of a nonconductive type. All unpainted metal surfaces on the main cylindrical section were electrically connected to a common spacecraft ground. The thermal control pattern resulting, therefore, allowed the possibility of small potential gradients across the spacecraft surface.

All portions of the solar array were treated with nonconductive paint with the exception of the soldered connections between the cells. These unpainted connectors had nominal dimensions of 10 cm × 1.52 cm each. The solar array was wired such that approximately 43 percent of the unpainted area of the array was below spacecraft potential, and approximately 57 percent was above spacecraft potential. This is illustrated in Fig. 16 where the spacecraft-space potential difference is plotted as a function of exposed solar array area which is above plasma potential.

All of the on-board experiment data is commutated for ground transmission. Ground transmission is accomplished with 350 mw at 136 MHz. With this system, the ambient probe data is sampled once every 4 minutes. This, coupled with the 106-minute orbital period, results in one ambient probe data point per 13° of geographic lattitude being obtained. Beam probe data is obtained once every 4 seconds that the probe is sweeping.

Thrusters

Two ion thrusters were on-board the spacecraft. Both systems were operated consecutively. The thrusters were of the Kaufman electron bombardment type, utilizing mercury as a propellant (Fig. 17). As shown in Fig. 1, the thrusters were canted a nominal 10° from the spacecraft longitudinal axis. Consequently, one thruster, when operating, raised the orbit by approximately 3.6 km/week. The other thruster, when operated, lowered the orbit by a similar amount. The majority of the data reported herein was obtained when the orbit raising thruster was operated.

The schematic of the thruster system is shown in Fig. 18. It shows the various power supplies necessary for operation of the thrusters. The thrust beam exits from the accelerating structure which consisted of a beam forming electrode and an acceleration electrode (Fig. 17). Each electrode contained 847 holes within a 15 cm diameter. There is no decelerating electrode. The electrons, necessary for neutralization of the ion beam, were obtained from the neutralizer located downstream of the accelerating structure. A perforated metal screen, at spacecraft potential, surrounded the thruster. This metal screen was within 1.2 cm of the neutralizer cathode tip.

The nominal potential profile of a thruster is shown in Fig. 19. The thruster normally produced a 253 mA ion beam at a nominal accelerating potential of 3000 V. However, each thruster was operated for short periods at 95 and 205 mA ion beam current.

The neutralizer was a plasma discharge device utilizing a hollow cathode.[3] The neutralizer was electrically isolated from the thruster system. A power supply (V_9) was provided to allow biasing the neutralizer relative to the spacecraft. This biasing supply was capable of changing the neutralizer-spacecraft potential difference, on command, from zero to a nominal ±25 or ±50 V. The supply was current limited at about 360 mA.

Appendix C

The equilibrium potential of a spacecraft in orbit will, in general, be different from that of the surrounding space plasma. Many factors affect the magnitude of the spacecraft potential. Among the more significant factors are:[9]

(a) Electron temperature, T_e

(b) Debye length

(c) Spacecraft-ion velocity ratio, $S_{S/C}/S_i$

(d) Ionic mass, M_i

(e) Electron and ion densities (ℓ_e and ℓ_i, respectively)

(f) V × B effects

(g) Exposed positive potentials

(h) Photoemission

(i) RF fields

For vehicles orbiting in the upper F_2-layer (≈1000 km), these factors generally result in a spacecraft potential negative with respect to the space plasma. This negative potential difference is usually on the order of several electron volts.[9] The exact value being dependent on the relative weights of the various effects. For such vehicles, in sunlight, generally the controlling factor on the potential is photoelectric emission from spacecraft surfaces.[9] However, it is shown that for the SERT II spacecraft, exposed surfaces at positive potentials seem to be the controlling factor on the equilibrium potential.

As inferred from the work of Bourdeau and Donley[15] and Whale[26], the effect of RF fields should be no greater than a few tenths of a volt with the SERT II spacecraft, the effect of RF was neglected.

For a spacecraft in orbit, neglecting RF, magnetic, and photoemission effects, equating of ion and electron currents require that

$$eA_iN_iS_{S/C} + eA_jN_iS_i = eA_eN_e\left(\frac{kT_e}{2\pi M_e}\right)^{1/2} \exp\left(\frac{-eV}{kT_e}\right) \quad (1)$$

where

A_e Effective electron collection area

N_i Ion number density

k Boltzmann constant

$S_{S/C}$ Spacecraft velocity

M_e Electron mass

S_i Ion velocity

V Spacecraft-space plasma potential difference

T_e Electron temperature

A_i Ram ion current collection area

N_e Electron number density

e Electron charge

T_e Electron temperature

A_j Thermal ion current collection area

The first term on the left side is the ram ion current. The second term is the thermal ion current. The term on the right side is the collected electron current. If charge and thermal equilibrium is assumed, then this reduces to

$$A_iS_{S/C} + A_jS_i = A_e\left(\frac{kT_e}{2\pi M_e}\right)^{1/2} \exp\left(\frac{-eV}{kT_e}\right) \quad (2)$$

Further, for a spacecraft moving with orbital velocity through the F_2-layer, $V_{S/C} \gg V_i$. Also, for the SERT II spacecraft, $A_j \simeq 4A_i$. Therefore, the above equation reduces to

$$A_iS_{S/C} = A_e\left(\frac{kT_e}{2\pi M_e}\right)^{1/2} \exp\left(\frac{-eV}{kT_e}\right) \quad (3)$$

For spacecraft potentials significantly (~10 kT_e/e) below plasma potential, the above equation reduces to

$$A_iS_{S/C} = A_e\left(\frac{kT_e}{2\pi M_e}\right)^{1/2} \quad (4)$$

or

$$A_e = \frac{A_iS_{S/C}}{\left(\frac{kT_e}{2\pi M_e}\right)^{1/2}} \quad (4a)$$

It is of interest to calculate the ram ion current. The ram ion current is given above by

$$J_i = A_iN_iS_{S/C}e \quad (5)$$

Now $A_i = 10.4\ M^2$ (Appendix B)

$N_i = 2\times10^4$ particles/cm^3 (Ref. 18)

$S_{S/C} = 7.35\times10^3$ M/sec

Therefore

$J_i = 0.24$ mA

References

1. Kerslake, W. R., Byers, D. C., and Staggs, J. F., "SERT II Experimental Thrustor System," Paper 67-700, Sept. 1967, New York, N.Y.

2. Sellen, J. M., Jr., "Interaction of Spacecraft Science and Engineering Subsystems with Electric Propulsion Systems," Paper 69-1106, Oct. 1969, AIAA, New York, N.Y.

3. Rawlin, V. K. and Kerslake, W. R., "Durability of the SERT II Hollow Cathode and Future Applications of Hollow Cathodes," Paper 69-304, Mar. 1969, AIAA, New York, N.Y.

4. Hall, D. F., Kemp, R. F., and Shelton, H., "Mercury Discharge Devices and Technology," Paper 67-669, Sept. 1967, AIAA, New York, N.Y.

5. Cole, R. K., Ogawa, H. S., and Sellen, J. M., Jr., "Operation of Solar Cell Arrays in Dilute Streaming Plasmas," Paper 69-262, Mar. 1969, AIAA, New York, N.Y.

6. Springgate, W. F., "High Voltage Solar Array Study," D2-121734-1, NASA CR-72674, 1970, The Boeing Company, Seattle, Wash.

7. Ogawa, H. S., Cole, R. K., and Sellen, J. M., Jr., "Measurements of Equilibration Potential Between a Plasma "Thrust" Beam and a Dilute "Space" Plasma," Paper 69-263, Mar. 1969, AIAA, New York, N.Y.

8. Sellen, J. M., Jr., "Study of Electric Spacecraft Plasmas and Field Interactions," Paper 69-276, Mar. 1969, AIAA, New York, N.Y.

9. Boyd, R. L. F., "The Direct Study of Ionization in Space," Advances in Atomic and Molecular Physics, Vol. 4, D. R. Bates and Immanuel Estermann, eds., Academic Press, New York, 1968, pp. 44σ-442.

10. Kemp, R. F. and Sellen, J. M., Jr., "Plasma Potential Measurements by Electron Emissive Probes," Review of Scientific Instruments, Vol. 37, No. 4, Apr. 1966, pp. 455-461.

11. Vernon, R. H. and Daley, H. L., "Emissive Probes for Plasma Potential Measurements on the SERT II Spacecraft," Paper 69-272, Mar. 1969, AIAA, New York, N.Y.

12. Henderson, C. L. and Samir, U., "Observations of the Disturbed Region Around an Ionospheric Spacecraft," Planetary and Space Science, Vol. 15, No. 10, Oct. 1967, pp. 1499, 1513.

13. Kerslake, W., Byers, D. C., Rawlin, V. K., Jones, S. G., and Berkopec, F. D., "Flight and Ground Performance of the SERT II Thruster," to be presented at the AIAA 8th Elec. Prop. Conf., 1970.

14. Samir, U. and Willmore, A. P., "The Equilibrium Potential of a Spacecraft in the Ionosphere," Planetary and Space Science, Vol. 14, No. 11, Nov. 1966, pp. 1131, 1137.

15. Bourdeau, R. E. and Donley, J. L., "Explorer VIII Satellite Measurements in the Upper Ionosphere," Proceedings of the Royal Society (London), Ser. A, Vol. 281, No. 1387, Oct. 6, 1964, pp. 487-504.

16. Krassovsky, V. I., "Exploration of the Upper Atmosphere with the Help of the Third Soviet Sputnik," IRE Proceedings, Vol. 47, No. 2, Feb. 1959, pp. 289-296.

17. Knudsen, W. C., "Geographic Distribution of F-Region Electrons With About 10-ev Energy," Journal of Geophysical Research, Vol. 73, No. 3, Feb. 1, 1968, pp. 841-856.

18. Brace, L. H., Reddy, B. M., and Mayr, H. G., "Global Behavior of the Ionosphere at 1000-Kilometer Altitude," Journal of Geophysical Research, Vol. 72, No. 1, Jan. 1, 1967, pp. 265-283.

19. Cybulski, R. J., Shellhammer, D. M., Lovell, R. R., Domino, E. J., and Kotnik, J. T., "Results from SERT I Ion Rocket Flight Test," TN D-2718, 1965, NASA, Cleveland, Ohio.

20. Hunter, R. E., Bartlett, R. O., Worleck, R. M., and James, E. L., "Cesium Contact Ion Microthruster Experiment Aboard Applications Technology Satellite (ATS)-IV," Journal of Spacecraft and Rockets, Vol. 6, No. 9, Sept. 1969, pp. 968-970.

21. Sellen, J. M., Jr. and Cybulski, R. J., "Environmental Effects on Laboratory and In-Flight Performance of Neutralizer Systems," Paper 65-70, Jan. 1965, AIAA, New York, N.Y.

22. Byers, D. C. and Snyder, A., "Parametric Investigations of Mercury Hollow Cathode Neutralizers," to be presented at the AIAA 8th Elec. Prop. Conf., 1970.

23. Chan, K. L. and Colin, L., "Global Electron Density Distributions From Topside Soundings," IEEE Proceedings, Vol. 57, No. 6, June 1969, pp. 990-1004.

24. Brace, L. H. and Findlay, J. A., "Comparison of Cylindrical Electrostatic Probe Measurements on Alouette II and Explorer XXXI Satellites," IEEE Proceedings, Vol. 57, No. 6, June 1969, pp. 1057-1060.

25. Hanson, W. B., "Structure of the Ionosphere," Satellite Environment Handbook, 2nd ed., F. S. Johnson, ed., Stanford University Press, 1965, pp. 21-49.

26. Whale, H. A., "The Excitation of Electro-acoustic Waves by Antennas in the Ionosphere," Journal of Geophysical Research, Vol. 68, No. 2, Jan. 15, 1963, pp. 415-422.

Spacecraft potential $V_{S/C}$, V	Electron collection area A_e, M^2	
	Measured	Calculated
-6.4	0.46	1.18
-8	.42	1.08

TABLE 1 CALCULATED AND MEASURED ELECTRON COLLECTION AREAS FOR TWO SPACECRAFT POTENTIALS

Position	Ion beam-neutralizer potential difference V_B, V		
	Ground test V	Northern hemisphere V	Southern hemisphere V
R = 0 cm (beam center)	61	67	62
R = 17 cm (Neut. position)	23	22	27

TABLE 2 ION BEAM-NEUTRALIZER POTENTIAL DIFFERENCE DURING FLIGHT AND GROUND TEST AT TWO BEAM POSITIONS

Ground Test Data				Flight Data								
V_9, V	$V_{S/C}$, V	V_B (max), V	I_5, mA	V_9, V	$V_{S/C}$ V		V_B (max), V		I_5, mA		I_9, mA	
52	-66	>38	250	52.0	-77.7	-75.1	>26.3	>28.9	258	253	258	250
26	-40	47	255	26.7	-46	-46	43.7	39	258	253	258	258
0	-14	47	250	0	-19.5	-19.5	46.4	41.6	258	253	258	258
0	---	---	205	0	-16.8	-16.8	37.2	-----	205	205	205	205
0	---	---	90	0	-16.8	-19.5	25.3	-----	95	95	94	95
0	0	0	0	0	-6.4	-9.0	0	0	0	0	0	0
-24	8	54.5	255	-22.6	-2.3	1.7	58.8	53.3	258	253	325	316
-39	22	64	255	-28.9	-0.9	7.0	65	63.4	258	258	343	343

TABLE 3 GROUND TEST AND FLIGHT NEUTRALIZER BIAS EXPERIMENT DATA. FLIGHT PARAMETER VALUES IN LEFT OF DOUBLE COLUMNS ARE FOR NORTHERN HEMISPHERE, RIGHT ARE FOR SOUTHERN HEMISPHERE

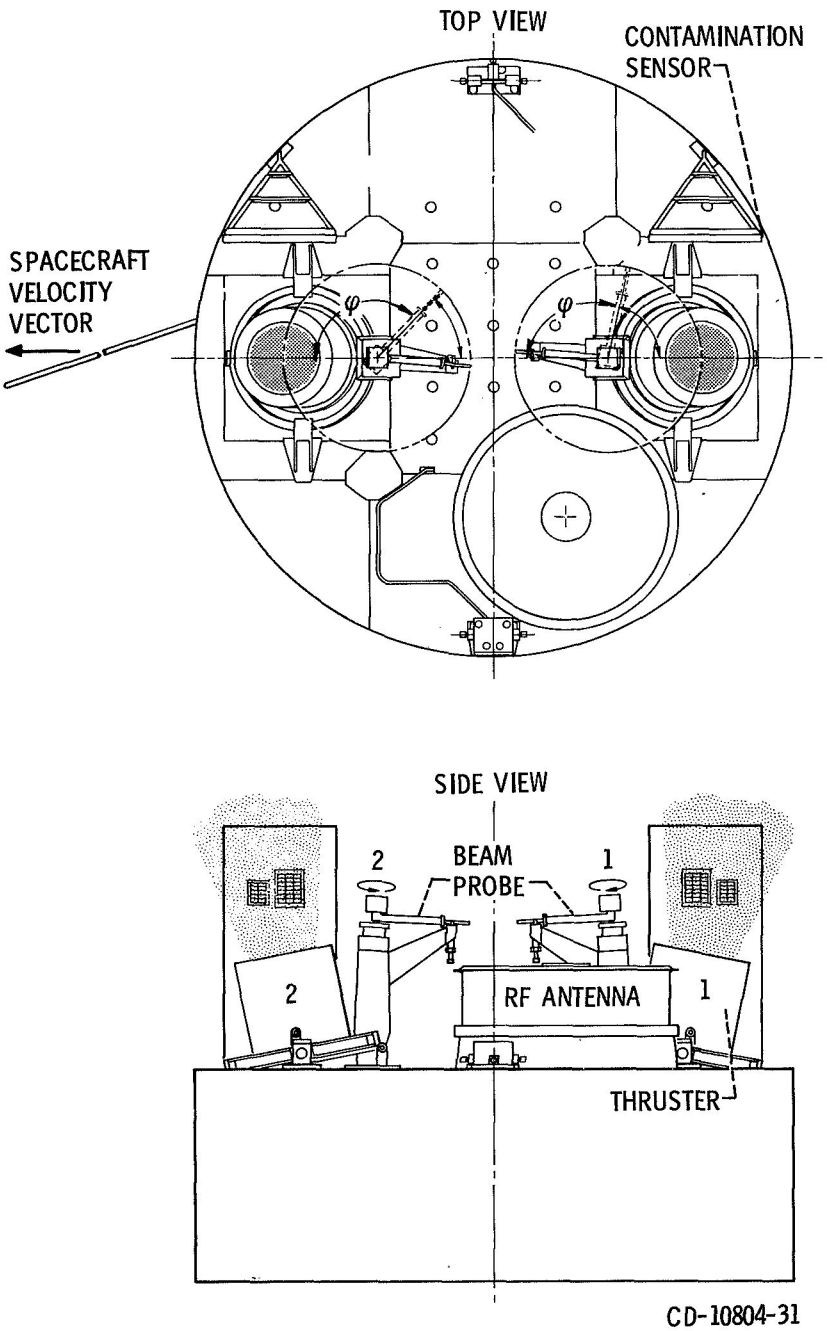

Figure 1. - SERT-II spacecraft.

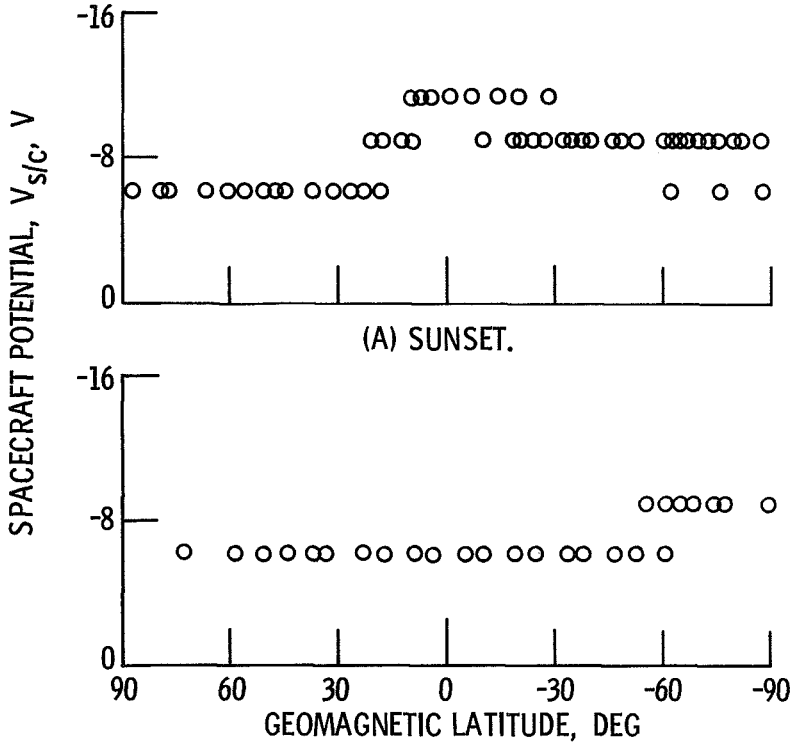

Figure 2. - Spacecraft potential as a function of geomagnetic latitude for sunrise and sunset. Passive spacecraft.

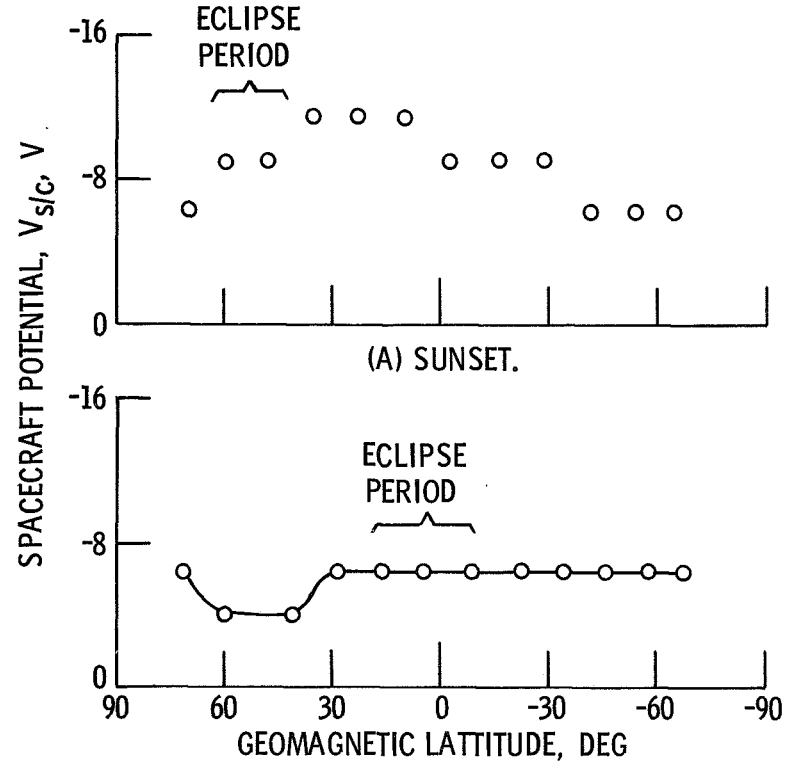

Figure 3. - Spacecraft potential as a function of geomagnetic latitude for sunset and sunrise showing eclipse data. Passive spacecraft.

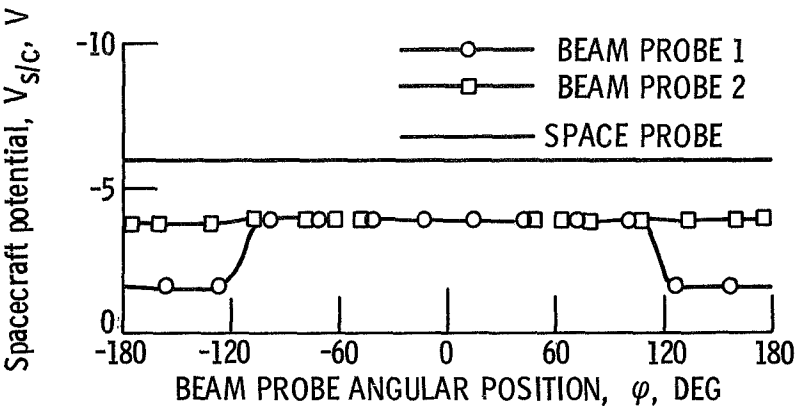

Figure 4. - Spacecraft potential as measured by the space probe and beam probe. Abscissa is the angle between the beam probe arm and the spacecraft velocity vector. Ion beam current, zero.

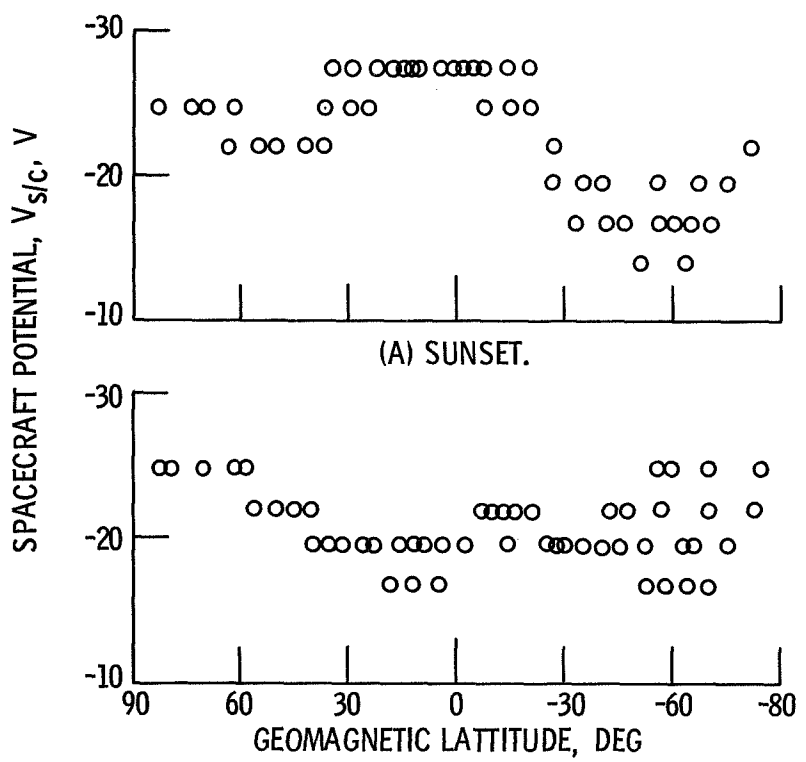

Figure 5. - Spacecraft potential as a function of geomagnetic lattitude for sunset and sunrise. Ion beam current 253 ma.

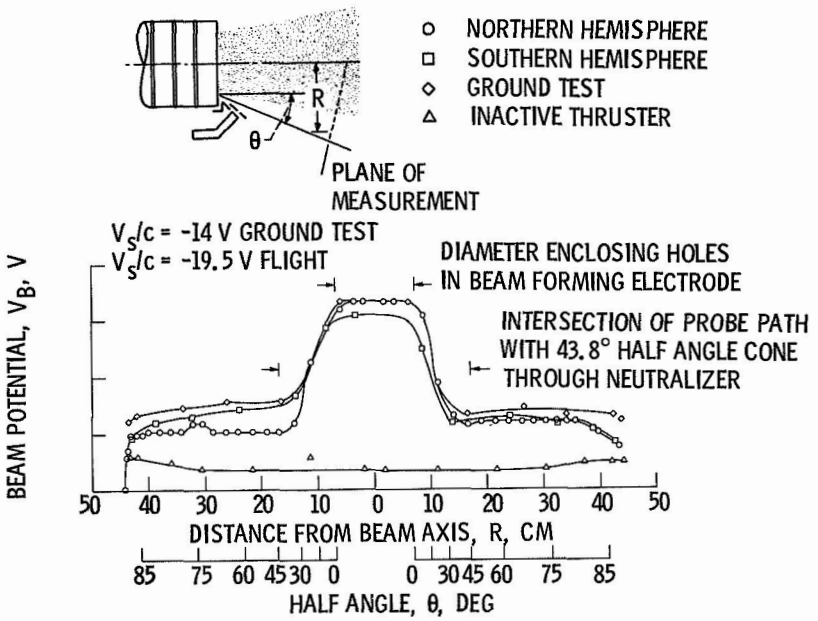

Figure 6. - Beam potential as a function of perpendicular distance from beam axis. Neutralizer bias zero. Ion beam current 250 ma.

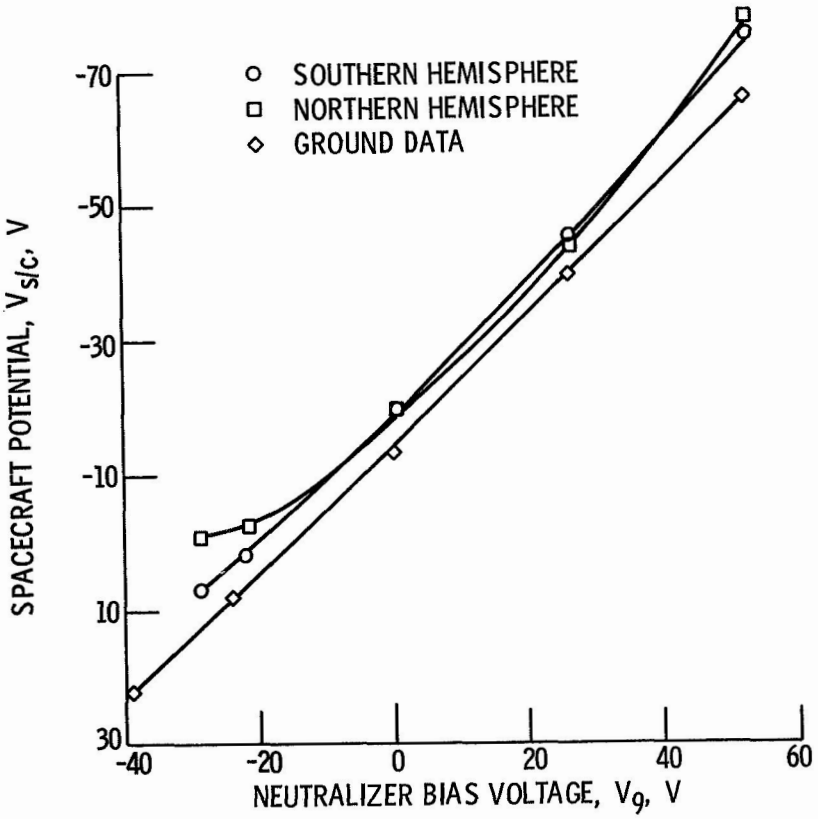

Figure 7. - Spacecraft potential as a function of neutralizer bias voltage. Ion beam current, I_S, 253 ma.

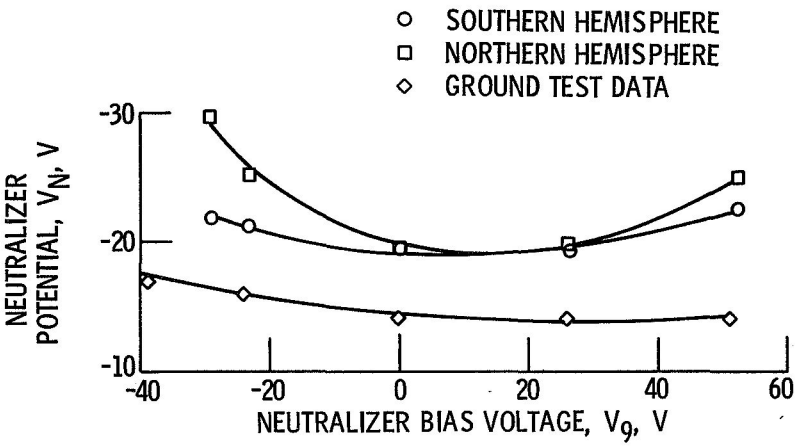

Figure 8. - Neutralizer potential as a function of neutralizer bias voltage for the northern and southern hemispheres. Ion beam current, I_5, 253 ma.

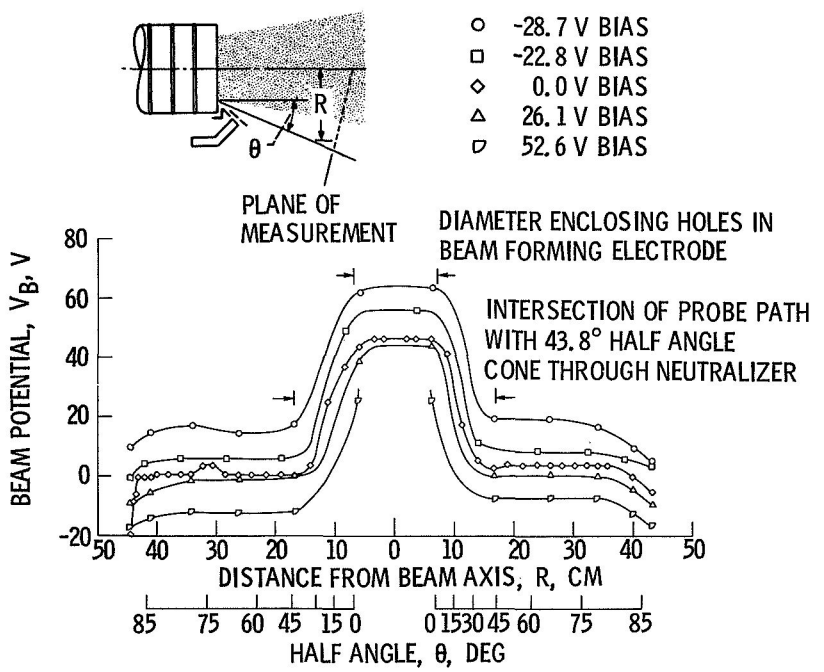

(A) NORTHERN HEMISPHERE.

Figure 9. - Beam potential as a function of perpendicular distance from beam axis in the northern hemisphere. Ion beam current, I_5, 253 ma.

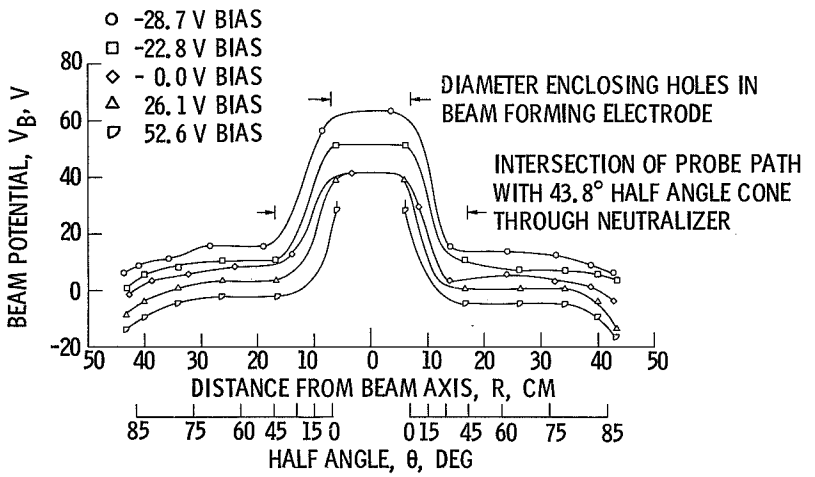

(B) SOUTHERN HEMISPHERE.

Figure 9. - Continued.

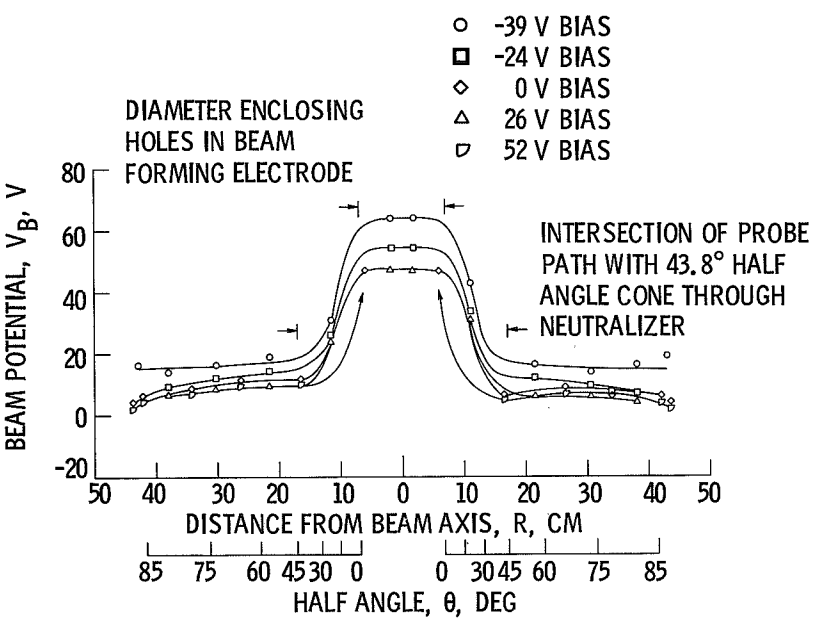

(C) GROUND TESTS.

Figure 9. - Concluded.

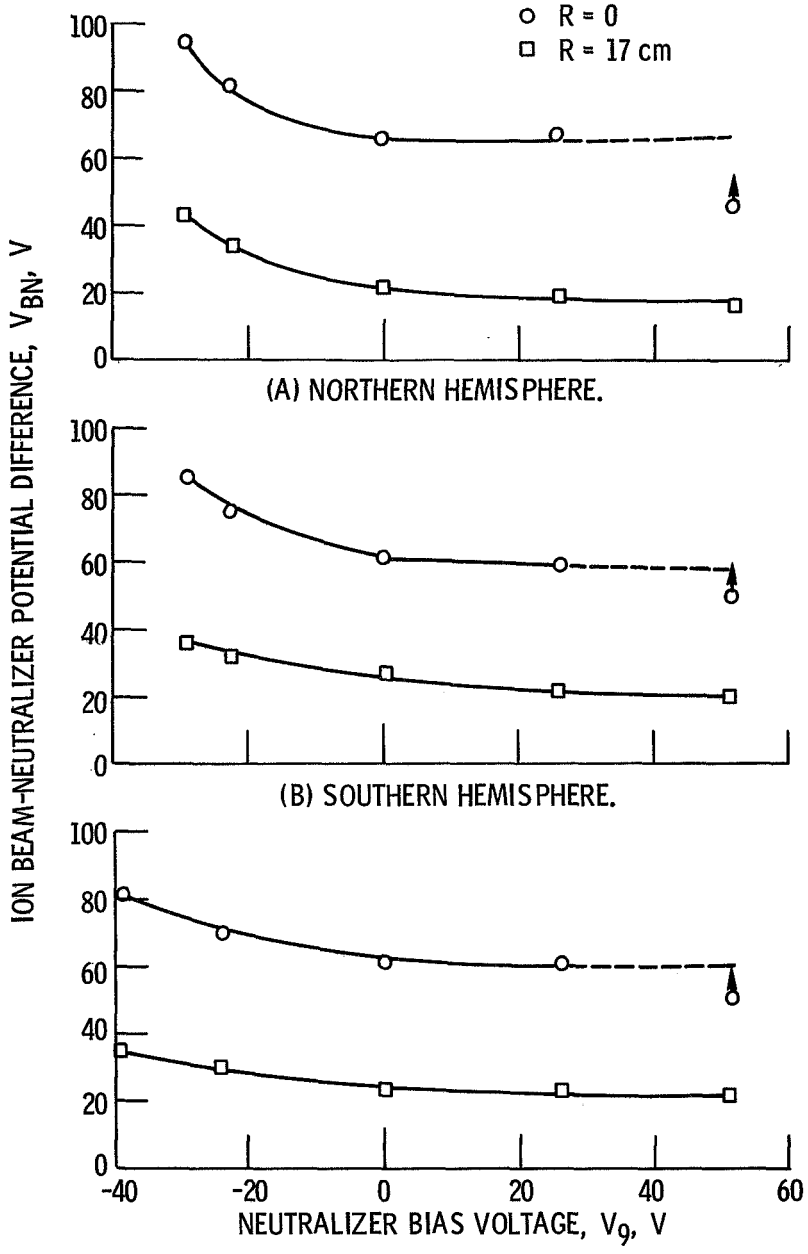

Figure 10. - Ion beam-neutralizer potential difference as a function of neutralizer bias voltage for the northern and southern hemispheres. Ion beam current, I_5, 253 ma.

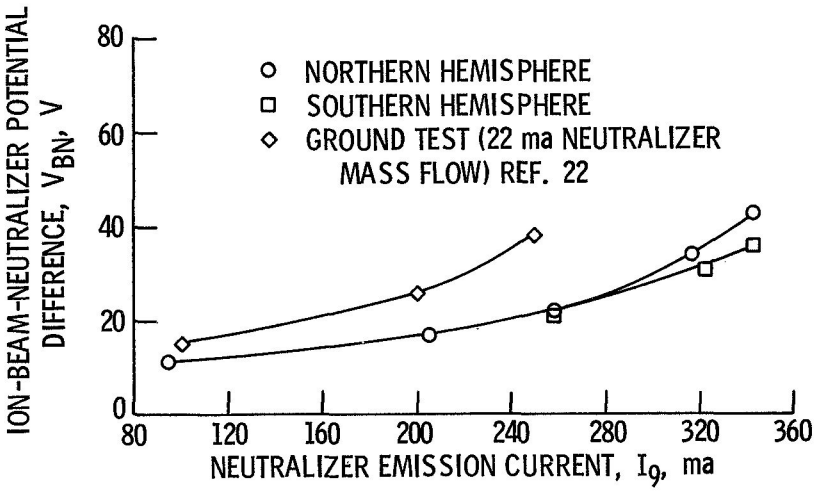

Figure 11. - Variation of ion beam-neutralizer potential difference with neutralizer emission current for R = 17 cm.

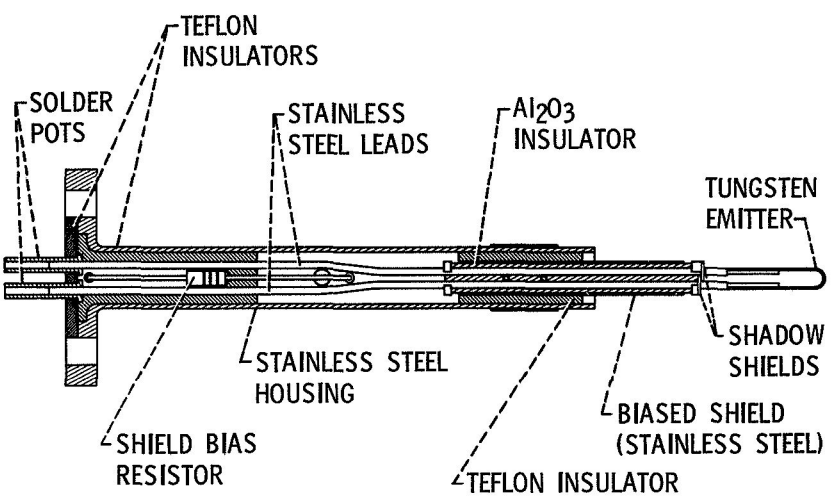

Figure 12. - Ambient probe emissive assembly.

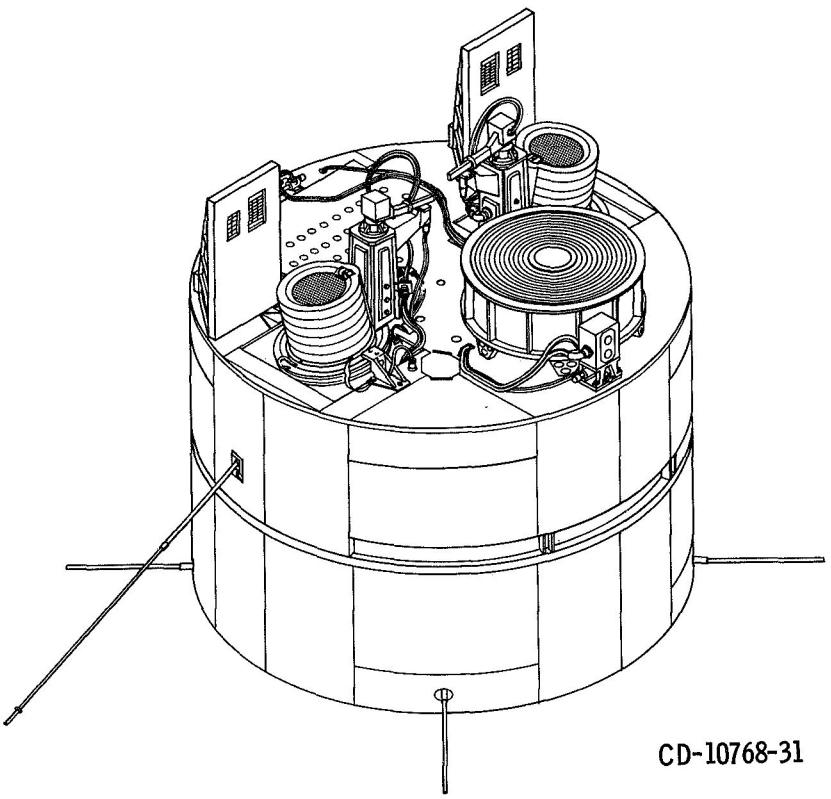

Figure 13. - SERT-II spacecraft.

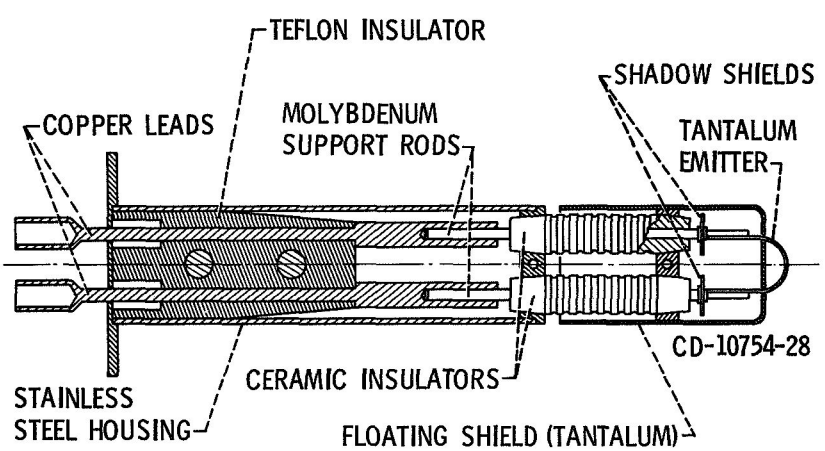

Figure 14. - Beam probe emissive assembly.

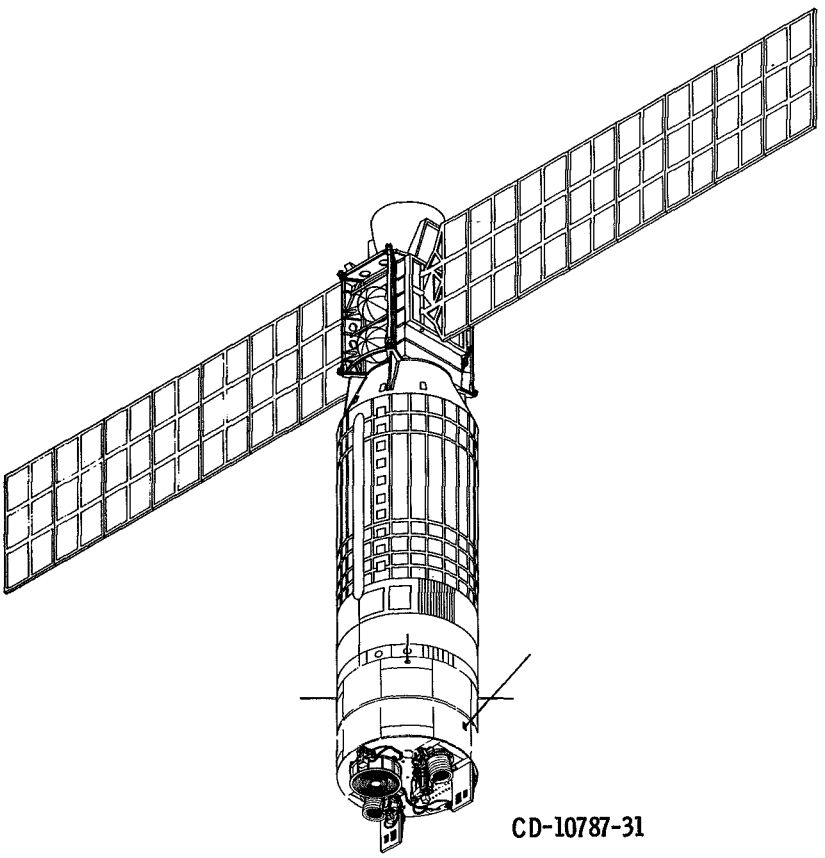

Figure 15. - SERT-II spacecraft in orbit (artist conception).

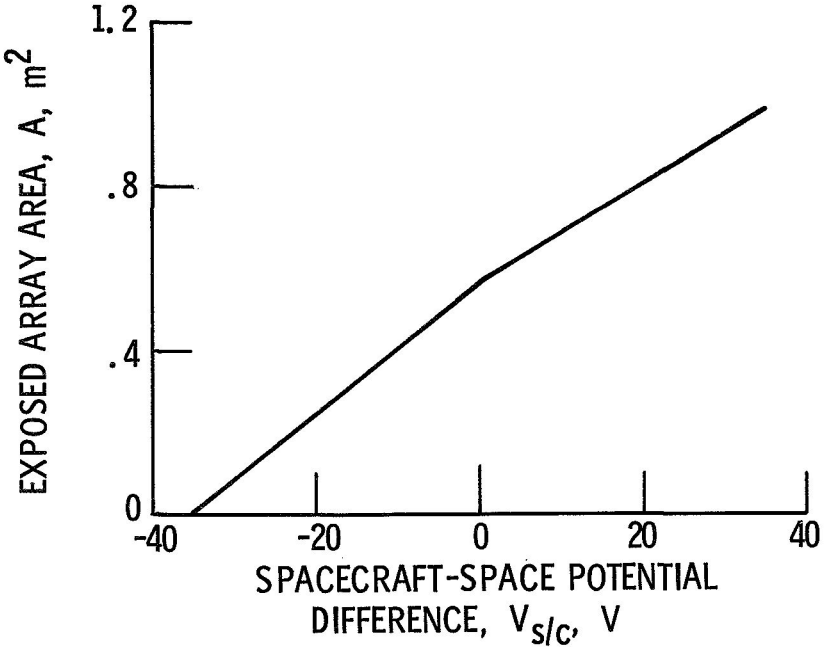

Figure 16. - Measured exposed solar array area as a function of spacecraft-space potential difference.

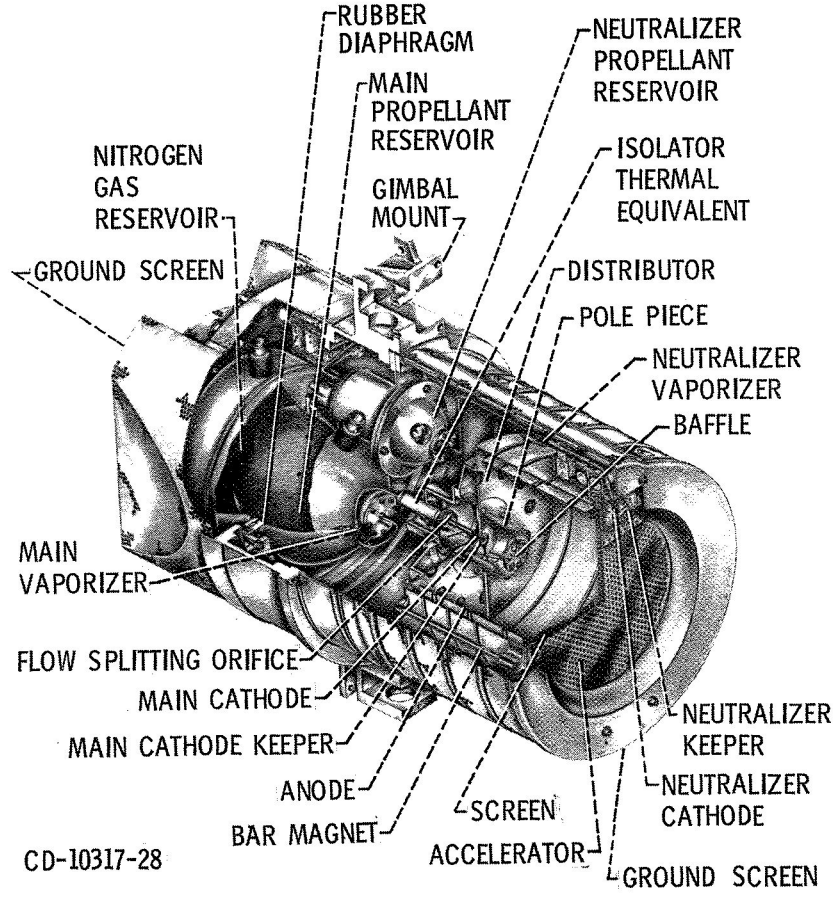

Figure 17. - SERT-II thruster.

V_2 MAIN VAPORIZER VOLTAGE
V_3 MAIN CATHODE VOLTAGE
V_4 MAIN ANODE VOLTAGE
V_5 SCREEN VOLTAGE
V_6 ACCELERATOR VOLTAGE
V_7 NEUTRALIZER CATHODE VOLTAGE
V_8 NEUTRALIZER ANODE VOLTAGE
V_9 NEUTRALIZER BIAS VOLTAGE
V_{10} MAIN KEEPER VOLTAGE

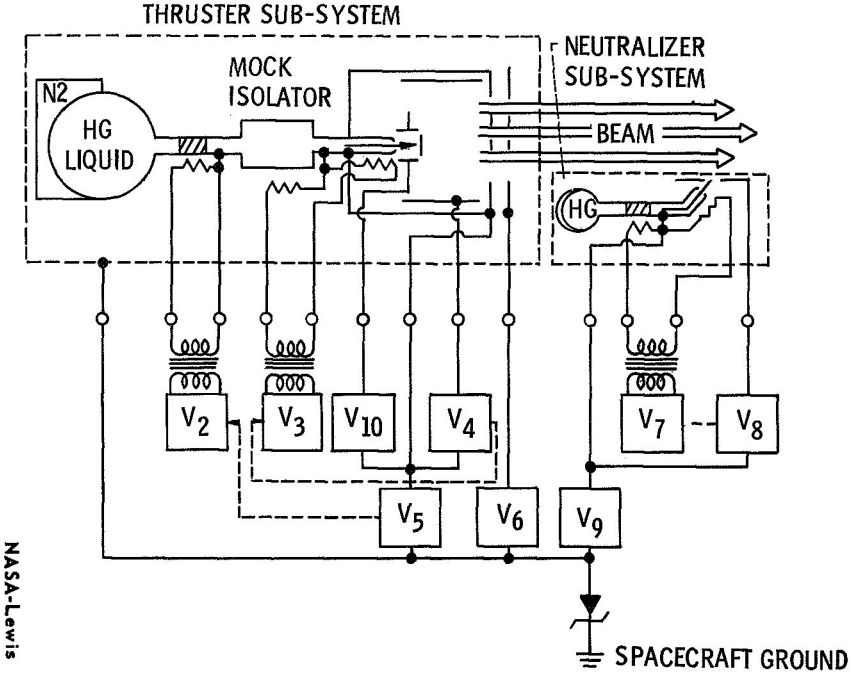

NASA-Lewis

Figure 18. - Electrical schematic of SERT II thruster.

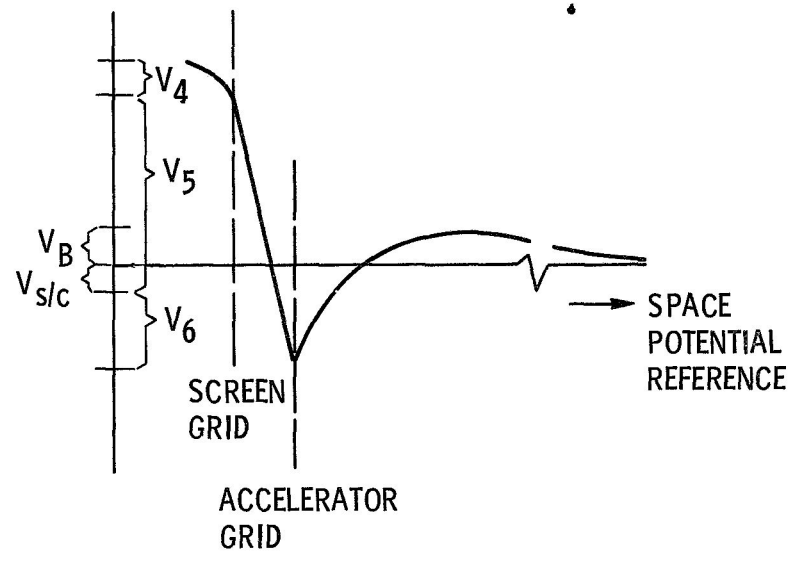

Figure 19. - SERT II ion thruster potential profile (not to scale).